Morphometric analysis of hard palate in Egyptian skulls

Saadia A. Shalaby, Esam M. Eid, Naglaa A.S. Sarg, Amany M.A. Sewilam

Department of Anatomy, Faculty of Medicine, Benha University, Benha, Egypt

Correspondence to Dr. Naglaa A. S. Sarg, MD, Department of Anatomy, Faculty of Medicine, Benha University, Benha, 13511, Egypt
Tel: 01225051719;
e-mail: naglasarg@hotmail.com

Received 02 May 2015
Accepted 06 May 2015

Benha Medical Journal
2015, 32:59–72

Background
As the hard palate is an essential region of the skull its gross anatomy and morphological variations have been of interest in many studies.

Aim
The aim of the present study was to describe the gross anatomy of the hard palate in Egyptian skulls, and determine sex from the morphometric study of the hard palate and location of the position of the greater palatine foramen (GPF) in relation to certain fixed intraoral anatomical reference points, all of which are visible or palpable in a living patient.

Materials and methods
In this study, 100 skulls (64 male and 36 female skulls) were subjected to the following measurements: palatal length, breadth, and height, the diameters of the GPF and its shape, the direction of opening of the GPF onto the palate, the relation of GPF to the maxillary molar teeth; the distance from the GPF to the midline maxillary suture, to the incisive foramen, to the posterior border of the hard palate, and to the tip of the hamular process of the pterygoid; the angle between the axis of the greater palatine canal (GPC) and the hard palate; the length of GPC plus the length of the pterygopalatine fossa; and the height of the maxilla. Twenty cadaveric heads were also dissected to measure the thickness of the palatal mucosa over the GPF.

Results
The mean palatal length was 51.65 ± 4.7 mm and palatal breadth was 38.68 ± 2.9 mm, with a highly significant difference between male and female skulls. Palatal height was 11.8 ± 2.7 mm with no significant difference between the two sexes. Of the total skulls 64% had narrow palates, 24% had intermediate ones, and 12% had wide palates with no significant difference between the two sexes; 36% had low palates, 56% had intermediate, and 8% of the sample had high-arched palates with a significant difference between the two sexes. The mean anteroposterior and transverse diameters of GPF were 4.86 ± 0.9 and 3.02 ± 0.7 mm, respectively. It was frequently an oval opening in 71%, a rounded opening in 22%, and lancet and slit in the remaining. Its direction in 69% was anteromedial, that in 28% was anterior, and that in 3% was anterolateral. The majority (84%) of the total foramina were opposite the maxillary third molar tooth. The mean distance from the GPF to the midline maxillary suture was 14.25 ± 1.7 mm, that from the GPF to the incisive foramen was 35.93 ± 3.5 mm, and that from the GPF to the posterior border of the hard palate was 3.89 ± 0.9 mm. The mean length of GPC and the pterygopalatine fossa was 29.39 ± 3.1 mm, the height of the maxilla was 30.44 ± 3.4 mm, and the difference between the two sexes was significant. The angle between the GPC and the horizontal plane of the hard palate was 40.48 ± 9.1°. The mean thickness of the palatal mucosa over the GPF was 4.92 ± 1.93 mm.

Conclusion
As the measurement studies of the hard palate show considerable variations among races, the data in this study will help clinicians to localize the GPF more precisely in Egyptian patients and to predict the depth of a needle to anesthetize the maxillary nerve with a low rate of complications.

Keywords:
hard palate, skull, morphometry, greater palatine framen

??? 32:59–72

????-????

Introduction

Measurement studies of the hard palate show considerable variation among races (Tables 1–4). Bone and dental structures of the palate are often preserved even in the face of serious bad damage at or following death. Sex determination using metric observation of the hard palate has been affirmed by Burris and Harris [1].

Metric studies of the hard palate help in accurate localization of the greater palatine foramen (GPF).

DOI: 10.4103/1110-208X.170560

Table 1 The palatine length, breadth, and height according to sex

Distance (mm)	Sex				Total (*N* = 100) $\bar{x}$ ± SD	*T* test	*P*
	Male (*N* = 64)		Female (*N* = 36)				
	Range	$\bar{x}$ ± SD	Range	$\bar{x}$ ± SD			
Palatine length	43.1–62.5	52.77 ± 5.16	46–54.3	49.66 ± 2.78	51.65 ± 4.7	3.92	<0.001
Palatine breadth	34–45	39.23 ± 3.02	35.1–42.3	37.71 ± 2.28	38.68 ± 2.9	2.84	<0.01
Palatine height	6–17	11.99 ± 3.04	8–14.1	11.6 ± 2.13	11.85 ± 2.7	0.75	>0.05

Table 2 The frequency of types of palate according to the palatine index in male and female skulls

Types	PI (%)	Male [*N* (%)]	Female [*N* (%)]	Total [*N* (%)]	*P*
Leptostaphyline	≤79.9	44/64 (68.8)	20/36 (55.6)	64/100 (64)	>0.05
Mesostaphyline	80–84.9	12/64 (18.8)	12/36 (33.3)	24/100 (24)	
Brachystaphyline	≥85	8/64 (12.5)	4/36 (11.1)	12/100 (12)	

PI, palatine index.

Table 3 The frequency of types of palate according to palatine height index in male and female skulls

Types	PHI (%)	Male [*N* (%)]	Female [*N* (%)]	Total [*N* (%)]	*P*
Chamestaphyline	≤27.9	28/64 (43.8)	8/36 (22.2)	36/100 (36)	<0.001
Orthostaphyline	28–39.9	28/64 (43.8)	28/36 (77.8)	56/100 (56)	
Hypsistaphyline	≥40	8/64 (12.5)	0/36 (0.00)	8/100 (8)	

PHI, palatine height index, which is the ratio of the palatine height to the palatine breadth expressed as a percentage; $P < 0.001$, highly significant.

Table 4 The anteroposterior diameter of the greater palatine foramen greater palatine foramen according to sex and side

GPF-diameter (mm)	Sex				Total ($\bar{x}$ ± SD)	*T* test	*P*
	Males		Females				
	Range	$\bar{x}$ ± SD	Range	$\bar{x}$ ± SD			
Right	3.9–6.5	4.94 ± 0.87	2.6–6	4.7 ± 1.04	4.86 ± 0.9	1.17	>0.05
Left	3.2–6.3	4.94 ± 1.06	2.6–6	4.49 ± 1.06	4.78 ± 1.01	1.9	>0.05
T	0.18		0.85		0.59		
P	>0.05		>0.05		>0.05		

GPF, greater palatine foramen.

Localization of the foramen is crucial in establishing local anesthesia by maxillary nerve block [2]. This approach has a high success rate with minimal risk [3]. A further advantage of this approach is the fact that the needle traverses the shortest route to block the maxillary nerve [4].

Blocking sensation of the maxillary nerve in the pterygopalatine fossa (PPF) achieves anesthesia of the maxillary teeth, the maxillary palate and gingival tissues, as well as the skin of the midface, nasal cavity, and sinus. Such a maxillary block would be necessary before various surgical procedures in this region, in patients with maxillary trauma, and for the diagnosis and treatment of chronic oral and maxillofacial pain syndromes. Furthermore, as simple infiltration into the buccal sulcus, adjacent to the tooth to be worked on, may be contraindicated in patients with an infection in the region, dentists may also need to resort to maxillary nerve blocks [5].

The aim of the present study is to describe the gross anatomy of the hard palate in Egyptian skulls, and determine sex from the morphometric study of the hard palate and location of the position of the GPF in relation to certain fixed intraoral anatomical reference points, all of which are visible or palpable in a living patient. The observations made in the present study were compared with those in earlier studies on skulls belonging to different races.

Materials and methods

This study was conducted on 100 adult Egyptian human dry skulls with or without mandibles. Sixty-four skulls were male and 36 were female. They were obtained from the Department of Human Anatomy in Benha Faculty of Medicine, Tanta Faculty of Medicine, Shebeen Elkoom Faculty of Medicine. The studied skulls were chosen so that the suture between the sphenoid and occipital bones (spheno-occipital suture) was obliterated. By the time there is obliteration of the spheno-occipital suture, the skull ages above 25 years old [6]. The selected skulls were without any anomalies, fractures or any pathology that might affect the normal measurements. Twenty cadavers were also dissected to measure the thickness of the palatal mucosa over the

GPF. All skulls were subjected to certain procedures that were performed bilaterally and directly on the dry skull by using the following tools: a caliper with 0.02 mm precision, a protractor, a compass, a ruler, a 25-G needle, and a rubber stop.

The following measurements and observations were recorded:

Each skull was measured for the following: palatal length, breadth, and height, which were measured to the nearest millimeter in the following manner. Length was the distance between the orale anteriorly (the orale is the point at the anterior end of the incisive suture located between the sockets of the two medial maxillary incisors) and the posterior nasal spine posteriorly. Width was the distance of the inner borders of the sockets of the upper second molars, endomolaria. Height was the distance of the maximum arching of the palate from the line connecting the two maxillary second molars, and hard palate was measured by using a ruler, needle, and caliper. The following indices were calculated according to the method followed by Hassanali and Mwaniki [7]: the palatine index (PI) and the palatine height index (PHI). The PI is the ratio of the palatine breadth to the palatine length expressed as a percentage. The values of the PI indicate the width of the palate. When the PI range was 79% or less, the hard palate was narrow (leptostaphyline); when the PI range was 80–84.9%, the hard palate was intermediate (mesostaphyline); and when the PI range was 85% or more, the hard palate was wide (brachystaphyline). The PHI is the ratio of palatine height to the palatine breadth expressed as a percentage. It indicates the characteristic arching of the palates. When the PHI was 27.9% or less, the hard palate was low (chamestaphyline); when it was 28–39.9%, the hard palate was intermediate (orthostaphyline); and when it was 40% or more, the hard palate was deep (hypsistaphyline).

The greater palatine foramen

Fixed intraoral reference points were identified and the distances of the GPF from these points were noted (Fig. 1). These reference points included the perpendicular distance from the medial edge of the foramen to the midline maxillary suture (MMS), the distance from the anterior edge of the foramen to the incisive fossa, and distances from the posterior edge of the foramen to the point of maximum concavity of the posterior palatal border and the pterygoid hamulus. Apart from this, the distance between the infraorbital foramen (IOF) and the alveolar crest between the maxillary premolars was measured, as it is a reliable indicator of the length of the greater palatine canal (GPC) and would thus help in judging the depth to which the needle should penetrate to reach the PPF through the GPF. Other metrical data included the sagittal dimensions of the GPF. Measurements were made using a vernier. Other parameters under which the GPF was studied included the following: the relation of the foramen to the maxillary molars; the angle between the axis of the GPC and the horizontal plane of the hard palate (Fig. 2); the angle made by the palatal midline and the line joining the GPF to the incisive foramen (IF) midline of the palate (GIM) angle; and the length of the GPC plus the length of the PPF, measured from the GPF to the inferior border of the foramen rotundum by using a 25-G needle with a rubber stop as a guide and caliper.

Figure 1

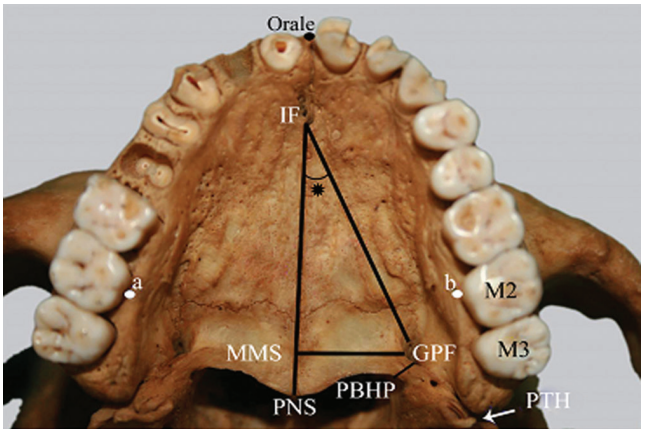

A photograph of the hard palate showing the following: the incisive foramen (IF); the greater palatine foramen (GPF); the posterior nasal spine (PNS); the midline maxillary suture (MMS); orale: the point at the anterior end of the incisive suture located between the sockets of the two maxillary central incisors; maxillary second molar (M2); maxillary third molar (M3); GPF-MMS: perpendicular distance from the GPF to the MMS; GPF-PBHP: distance from the GPF to the posterior border of the hard palate. * indicates angle between the MMS and the line from the IF and the GPF; a, b: palatine breadth.

Torus palatinus is a bony protrusion on the palate usually present on the midline of the hard palate. Although some researchers suggest palatal tori to be an autosomal dominant trait, it is generally believed that palatal tori are caused by several factors. They are more common in early adult life and can increase in size. In some older people, the size of the tori may decrease because of bone resorption. The tori are categorized by their appearance, which can be in ridge form – relatively narrow and uniform in width – a mound – relatively wide and tapering anteriorly and posteriorly – and a lump form – irregular in shape [8].

The length (from the beginning to the end along the median palatine suture), breadth (at the widest part), and height of the palatine torus if present were

measured. The form of the palatine torus was evaluated as a ridge, mound, or lump.

Twenty cadaveric heads (unknown sex) were also dissected to measure the thickness of the palatal mucosa over the GPF.

Statistical analysis

All distances were measured with vernier calipers to the nearest millimeter. All measurements and frequencies of the data were tabulated and separated according to the side and gender. Basic descriptive statistics were employed to analyze the data using SPSS (SPSS Inc., Chicago, Illinois, USA). The mean, SD, and range for each of the measurements were assessed. Comparison of the values of all measurements was made in terms of the sides in each subject, as well as comparisons between sexes.

Results

One hundred adult Egyptian skulls, 64 male and 36 female, were examined. Each skull was subjected to the observations and measurements mentioned earlier. The thickness of the palatal mucosa over the GPF in 20 cadaveric heads was measured. Basic descriptive statistics were used to analyze the obtained data.

The palatal length, breadth, and height

The mean palatal length was 52.77 ± 5.16 mm in male skulls, 49.66 ± 2.78 mm in female skulls, and 51.65 ± 4.7 mm in the total sample. Mean palatal breadth was 39.23 ± 3.02 mm in male skulls, 37.71 ± 2.28 mm in female skulls, and 38.68 ± 2.9 mm in the total sample. Mean palatal height was 11.99 ± 3.04 mm in male skulls, 11.6 ± 2.13 mm in female skulls, and 11.8 ± 2.7 mm in the total sample. The statistical analysis of these data indicated that there was a highly significant difference between male and female skulls as regards the palatal length ($P < 0.001$), the palatal breadth ($P < 0.01$), and the arching of the palate ($P < 0.001$). However, as regards the palatal height the difference between male and female skulls was insignificant ($P > 0.05$) (Table 1).

Types of palate

From the palatal length and breadth of each skull, the PI, which is the ratio of the palatine breadth to the palatine length, expressed as a percentage, was calculated and its values indicated that the percentage of narrow palate (leptostaphyline) was 68.8% in male skulls, 55.6% in female skulls, and 64% in total skulls (Figs 3, 4, and 5). The percentage of the intermediate palate (mesostaphyline) was 18.8% in male skulls, 33.3% in female skulls, and 24% in the total skulls (Figs 6, 7, and 8). The percentage of the wide palate (brachystaphyline) was 12.5% in male skulls, 11.1% in female skulls, and 12% in total skulls (Figs 9 and 10), with no significant difference between the two genders ($P > 0.05$) (Table 2).

Arching of the palate

The PHI was calculated from the palatal breadth and height and its values indicated that the percentage of the low or flat palate (chamestaphyline) was 43.8% in male skulls, 22.2% in female skulls, and 36% in the total sample (Figs 8 and 9). The percentage of the intermediate arching palates (orthostaphyline) was 43.8% in male skulls, 77% in female skulls, and 56% in total skulls (Figs 6, 7, and 11). The percentage of

Figure 2

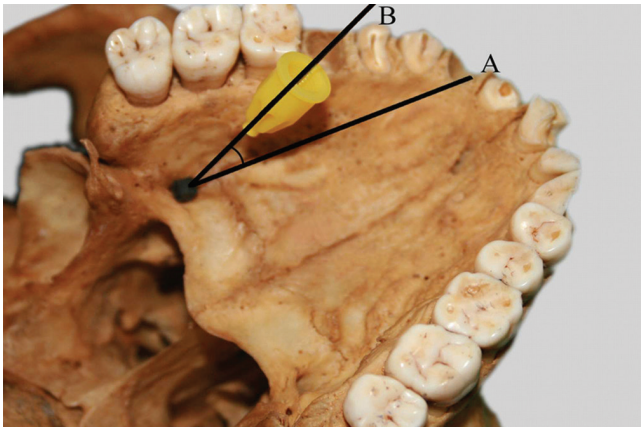

A photograph of a hard palate showing the angle between the axis of the greater palatine canal (B) and the anteroposterior plane of the hard palate (A).

Figure 3

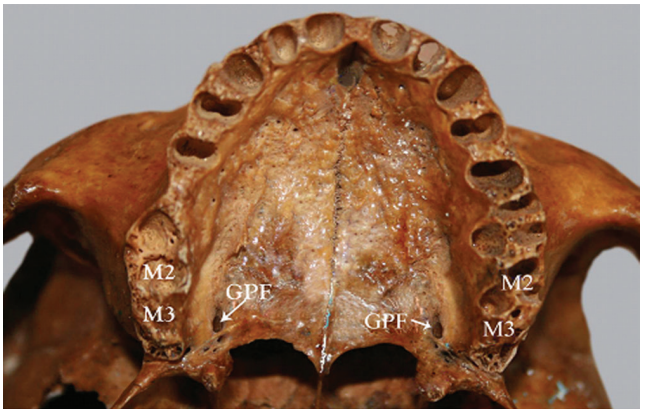

A photograph of an adult male skull: The hard palate is narrow (leptostaphyline) and intermediate in arching (orthostaphyline). The greater palatine foramen (GPF) lies opposite the third molar (M3) and is oval in shape. M2, second molar.

Figure 4

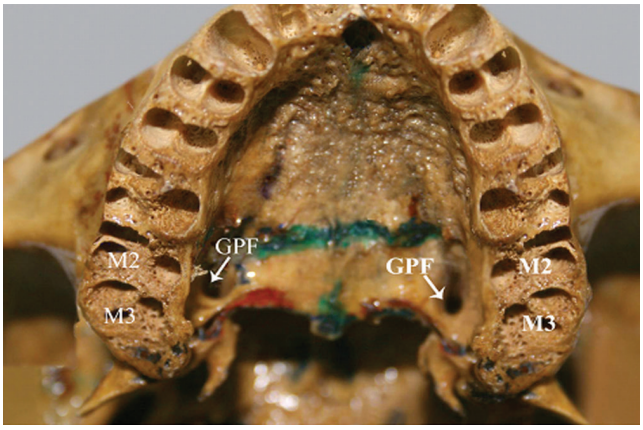

A photograph of adult male skull. The hard palate is narrow (leptostaphyline) and deep (hypsistaphyline). The greater palatine foramen (GPF) lies between the third molar (M3) and the second molar (M2) and is rounded in shape.

Figure 5

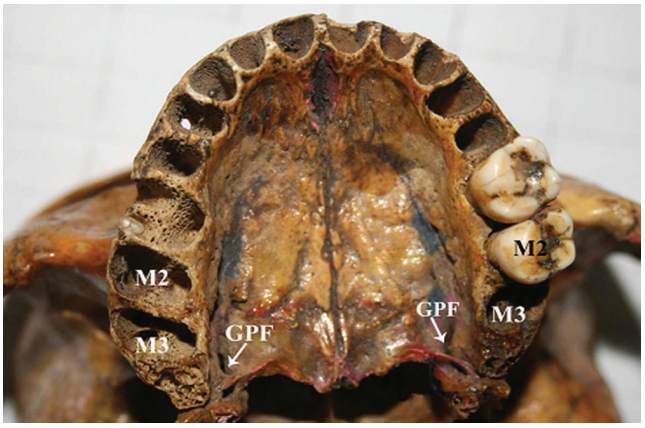

A photograph of an adult male skull. The hard palate is narrow (leptostaphyline) and intermediate in arching (orthostaphyline). The greater palatine foramen (GPF) lies behind the third molar (M3) and is slit in shape. M2, second molar.

Figure 6

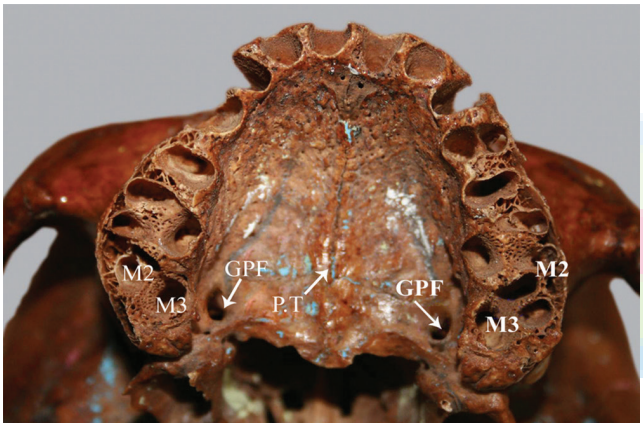

A photograph of an adult female skull. The hard palate is intermediate (mesostaphyline) and intermediate in arching (orthostaphyline). The greater palatine foramen (GPF) lies opposite the third molar (M3) and is lancet in shape. Note a palatine torus (PT) along the interpalatine suture. M2, second molar.

Figure 7

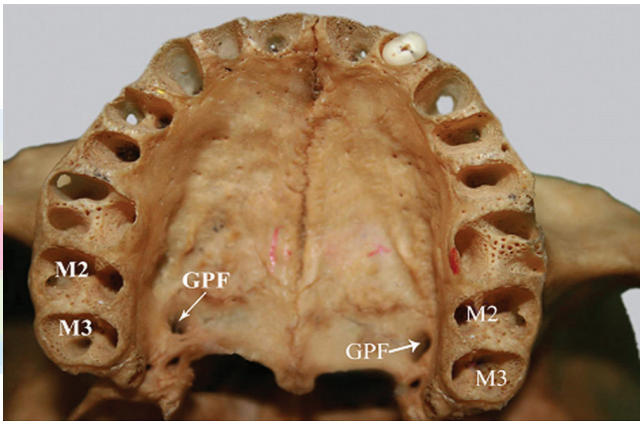

A photograph of an adult male skull. The hard palate is intermediate (mesostaphyline) and intermediate in arching (orthostaphyline). The greater palatine foramen (GPF) lies between the third molar (M3) and the second molar (M2), especially on the left side, and is rounded in shape on the right side and oval in shape on the left side.

the high-arched palates (hypsistaphyline) was 12.5% in male skulls, 0% in female skulls, and 8% in total skulls (Fig. 4). There was a highly significant difference between the two genders ($P < 0.001$) (Table 3).

The greater palatine foramen

As regards the GPF, it was present bilaterally, one on each side on the posterolateral aspect of the hard palate in all skulls. The mean of the anteroposterior diameter of this foramen was 4.94 ± 0.87 and 4.94 ± 1.06 mm for right and left sides, respectively, in male skulls, 4.7 ± 1.0 and 4.49 ± 1.06 mm for right and left sides, respectively, in female skulls, and 4.86 ± 0.9 and 4.78 ± 1.01 mm for right and left sides, respectively, in total skulls (Table 4).

The mean of the transverse diameter of the GPF was 3.25 ± 0.7 and 3.28 ± 0.9 mm for right and left sides, respectively, in male skulls, 2.6 ± 0.4 and 2.46 ± 0.5 mm for right and left sides, respectively, in female skulls, and 3.02 ± 0.7 and 3.01 ± 0.9 mm for right and left sides, respectively, in total skulls (Table 5).

The GPF was frequently found as an oval opening in 71 and 69% of total skulls for the right and left sides, respectively (Figs 3 and 7). A rounded opening was found in 22 and 25% of total skulls for right and left sides, respectively (Figs 4 and 7). A lancet shape was found in 5 and 4% of the total foramina for right and left sides, respectively (Fig. 6) and a slit shape was seen in 2% of male skulls on the right and left sides and was not found in female skulls (Fig. 5). *P* values were

Table 5 The transverse diameter of greater palatine foramen according to sex and side

GPF-transverse diameter (mm)	Sex				Total ($\bar{x}$ ± SD)	*T* test	*P*
	Males		Females				
	Range	$\bar{x}$ ± SD	Range	$\bar{x}$ ± SD			
Right	2–5	3.25 ± 0.7	2.2–3.5	2.6 ± 0.4	3.02 ± 0.7	5.73	<0.001
Left	2–5.5	3.28 ± 0.9	2–3.5	2.46 ± 0.5	3.01 ± 0.9	5.86	<0.001
T test		0.21		1.49	0.09		
P		>0.05		>0.05	>0.05		

GPF, greater palatine foramen.

Figure 8

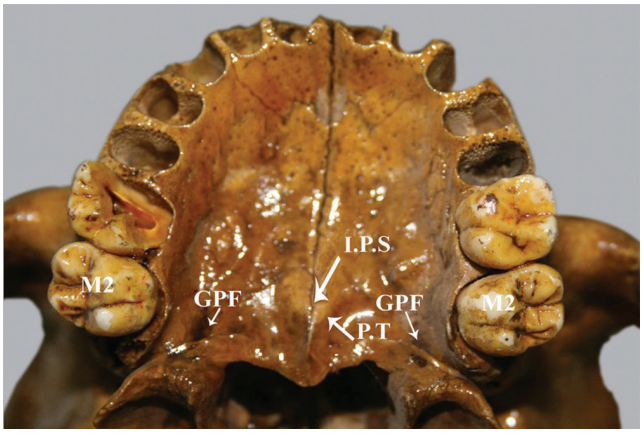

A photograph of an adult male skull. The hard palate is intermediate (leptostaphyline) and flat (chamestaphyline). The greater palatine foramen (GPF) is located opposite the second molar (M2). Note a palatine torus (PT) along the interpalatine suture (IPS) in mound form.

Figure 9

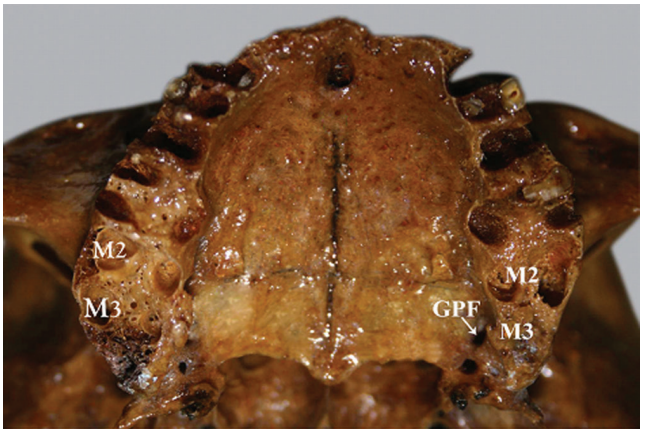

A photograph of an adult male skull: The hard palate is wide (brachystaphyline) and flat (chamestaphyline). The greater palatine foramen (GPF) lies opposite the third molar. M2, second molar; M3, third molar.

Figure 10

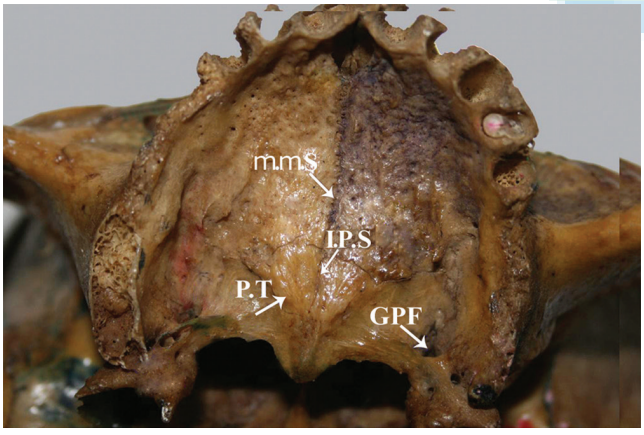

A photograph of an adult male skull. The hard palate is wide (brachystaphyline) and flat (chamestaphyline).The palatine torus (PT) is along the interpalatine suture (IPS) and the posterior part of the midline maxillary suture (MMS) is in mound form.

Figure 11

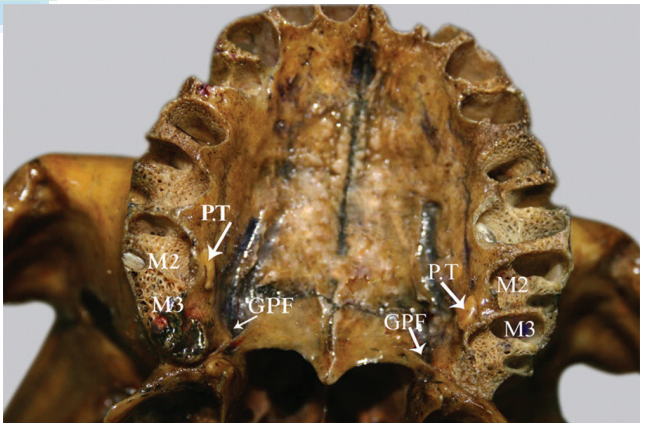

A photograph of an adult male skull. The hard palate is narrow (leptostaphyline) and intermediate in arching (orthostaphyline). The greater palatine foramen (GPF) is behind the third molar. M2, second molar; M3, third molar; PT, palatine torus.

greater than 0.05 between the two sexes in terms of the frequency of the shape of the foramen (Table 6).

The GPF was opened in an oblique direction; it was forward and medial in 69% (Fig. 12), forward in 28% (Fig. 13), and forward and lateral in 3% (Fig. 14). The direction in male skulls was forward and medial in 67.2%, forward in 29.7%, and forward and lateral in 3.1%. In female skulls, the direction was forward and medial in 72.2%, forward in 25%, and forward and lateral in 2.8%; this also represented the direction of the GPC. No foramina

Figure 12

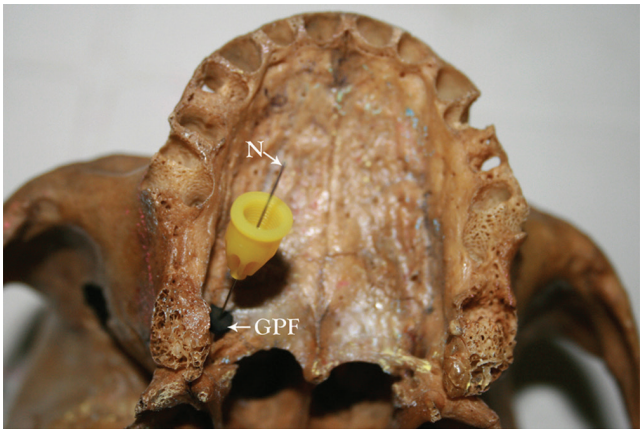

A photograph of an adult male skull. The direction of the needle (N) inserted into the greater palatine canal through the greater palatine foramen (GPF) is forward and medial.

Figure 13

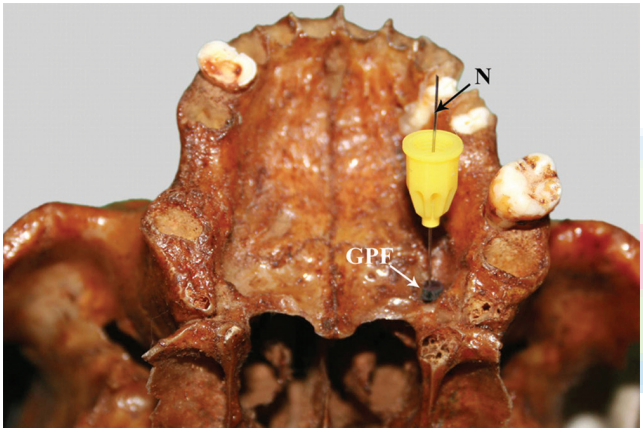

A photograph of an adult female skull. The direction of the needle (N) inserted into the greater palatine canal through the greater palatine foramen (GPF) is forward.

Figure 14

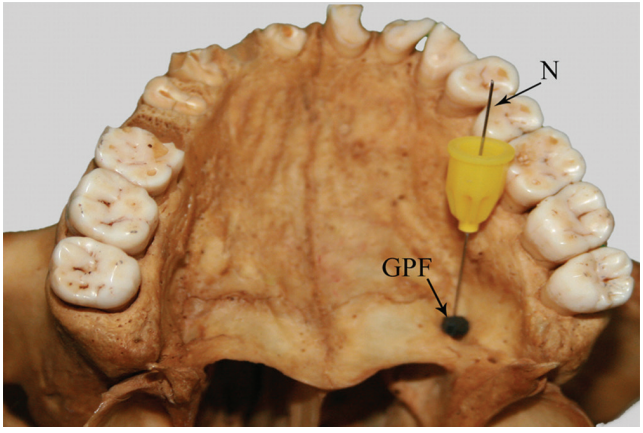

A photograph of an adult male skull. The direction of the needle (N) inserted into the greater palatine canal through the greater palatine foramen (GPF) is forward and lateral.

opened in a perpendicular, downward (vertical) direction (Table 7).

The GPF was opposite the maxillary third molar in 82.8, 86.1, and 84% of male, female, and total skulls, respectively (Figs 3–9). The foramen was between the maxillary second and third molars in 9.4, 8.3, and 9% of male, female, and total skulls (Figs 4 and 7). The foramen was distal to the maxillary third molar in 6.3, 5.6, and 6% of male, female, and total skulls, respectively (Figs 5 and 11). Only in 1% of the total skulls (a male skull) was it opposite the maxillary second molar (Fig. 8). This was the same on both sides (Table 8).

The mean distance from the GPF to the MMS was 14.87 ± 1.4 and 14.97 ± 1.2 mm on right and left sides, respectively, in male skulls, 13.94 ± 2.1 and 13.96 ± 2.2 mm on right and left sides, respectively, in female skulls, and 14.25 ± 1.7 and 14.17 ± 1.6 mm on right and left sides, respectively, in total skulls (Table 9).

The mean distance from the center of the GPF to the posterior border of the IF was 37.09 ± 3.3 and 37.08 ± 3.7 mm on right and left sides, respectively, in male skulls, 33.87 ± 2.89 and 34.19 ± 2.89 mm on right and left sides, respectively, in female skulls, and 35.93 ± 3.5 and 36.04 ± 3.7 mm on right and left sides, respectively, in total skulls (Table 10).

The mean distance from the center of the GPF to the posterior border of the hard palate was 4.17 ± 0.94 and 4.2 ± 0.95 mm on right and left sides, respectively, in male skulls, 3.39 ± 0.7 and 3.61 ± 0.7 mm on right and left sides, respectively, in female skulls, and 3.89 ± 0.9 and 3.99 ± 0.9 mm on right and left sides, respectively, in total skulls (Table 11).

The mean distance from the center of the GPF to the tip of the hamular process of the pterygoid process was 12.29 ± 2.57 and 12.38 ± 2.45 mm on right and left sides, respectively, in male skulls, 11.66 ± 1.57 and 11.51 ± 1.95 mm on right and left sides, respectively, in female skulls, and 12.06 ± 2.3 and 12.07 ± 2.2 on right and left sides, respectively, in total skulls (Table 12).

The GIM angle, the angle between the MMS and the line from the IF and the GPF, was 23.3 ± 4.5 and 23.6 ± 3.9° on right and left sides, respectively, in male skulls, 22.9 ± 4.4 and 23.1 ± 4.4° on right and left sides, respectively, in female skulls, and 22.9 ± 4.4 and 23.2 ± 4.1° on right and left sides, respectively, in total skulls (Table 13).

The angle of the GPC, formed between the long axis of the needle in the GPC and the horizontal plane of the hard palate, was measured whenever the needle was angled toward the anterior portion of the palate. The

Table 6 The percentage of different shapes of greater palatine foramen according to sex and side

GPF shapes	Male [*N* (%)]		Female [*N* (%)]		Total [*N* (%)]	
	Right	Left	Right	Left	Right	Left
Oval	45 (70.31)	44 (68.75)	26 (72.22)	25 (69.44)	71 (71.00)	69 (69.00)
Rounded	14 (21.88)	16 (25.00)	8 (22.22)	9 (25.00)	22 (22.00)	25 (25.00)
Lancet	3 (4.69)	2 (3.13)	2 (5.56)	2 (5.56)	5 (5.00)	4 (4.00)
Slit	2 (3.13)	2 (3.13)	0 (0.00)	0 (0.00)	2 (2.00)	2 (2.00)
N	64	64	36	36	100	100

GPF, greater palatine foramen.

Table 7 The direction of opening of the greater palatine foramen onto the palate according to sex

Sex	GPF [*N* (%)]			
	Forward and medial	Forward	Forward and lateral	Vertical
Male	86 (67.2)	38 (29.7)	4 (3.1)	0 (0.0)
Female	52 (72.2)	18 (25.0)	2 (2.8)	0 (0.0)
Total	138 (69.0)	56 (28.0)	6 (3.0)	0 (0.0)

GPF, greater palatine foramen.

Table 8 The relation of the greater palatine foramen to the maxillary molars according to sex

Sex	GPF [*N* (%)]			
	Opposite M3	Between M3 and M2	Behind M3	Opposite M2
Male	106 (82.8)	12 (9.4)	8 (6.3)	2 (1.6)
Female	62 (86.1)	6 (8.3)	4 (5.6)	0 (0.0)
Total	168 (84.0)	18 (9.0)	12 (6.0)	2 (2.0)

GPF, greater palatine foramen; M2, second molar; M3, third molar.

mean angle was 40.81 ± 9.1 and 40.69 ± 9.1° on right and left sides, respectively, in male skulls, 39.89 ± 9.4 and 39.33 ± 9.4° on right and left sides, respectively, in female skulls, and 40.48 ± 9.1 and 40.2 ± 9.2° on right and left sides, respectively, in total skulls (Table 14).

As regards the length of the GPC and the PPF, the mean length was 29.83 ± 3.2 and 29.99 ± 3.27 mm on right and left sides, respectively, in male skulls, 28.61 ± 2.8 and 28.63 ± 2.9 mm on right and left sides, respectively, in female skulls, and 29.39 ± 3.1 and 29.5 ± 3.2 mm on right and left sides, respectively, in total skulls (Table 15).

The distance between the lower border of the IOF and the alveolar crest between the maxillary premolars was measured. The mean length was 31.36 ± 3.37 and 31.63 ± 3.1 mm on right and left sides, respectively, in male skulls, 28.82 ± 2.71 and 29.63 ± 2.5 mm on right and left sides, respectively, in female skulls, and 30.44 ± 3.4 and 30.91 ± 3.1 mm on right and left sides, respectively, in total skulls. Statistical analysis indicated that there was no significant difference between right and left sides (P>0.05) but the difference between the two sexes was highly significant (P < 0.001) (Table 16).

Statistical analysis revealed no significant difference in the measurements of the GPF to the intraoral landmarks between the right and left sides. Also there was no significant difference between male and female skulls in the anteroposterior diameters of the GPF, the distance from GPF to the tip of the hamular process of the pterygoid process, value of GIM, and the position of GPF to the third molar.

However, the difference between the two sexes was found to be significant for the distance between GPF and the MMS (P < 0.05) and length of GPC and PPF (P < 0.05), and highly significant for the distance from the center of the GPF to the posterior border of the IF (P < 0.001), from the GPF to the posterior palatal border (P < 0.001), and the distance from the IOF to the alveolar crest between the two maxillary premolars (P < 0.001).

As far as the patency of the GPF is concerned, a 25-G needle was passed through the GPF without difficulty into the PPF with a patency rate of 100%, as none of the examined skulls showed anatomical obstruction while attempting to insert the needle to reach the foramen rotundum through the GPC.

Palatine torus was observed in 7% of total skulls, 6.25% of male skulls, and 8.3% of female skulls. The mean of the length of the torus was 20.6 ± 7.8 mm in total skulls, 22.5 ± 10.5 mm in male skulls, and 18 ± 1.7 mm in female skulls. The mean width of the palatine tori was 10.5 ± 4.5 mm in total skulls, 9.9 ± 4.4 mm in male skulls, and 11.3 ± 5.5 mm in female skulls. The mean height of the palatine torus was 4.1 ± 1.2 mm in total skulls, 4.8 ± 1.3 mm in male skulls, and 3.3 ± 0.58 mm in female skulls. There was no statistical significant difference between the two sexes (Table 17).

The palatine tori (Figs 6 and 15) appeared in ridge form (Figs 8 and 10), mound form (Fig. 16), and lump form (Table 18).

The palatine torus was located along the midsagittal line of the hard palate and did not deviate from this line. The most common position of the palatine tori was the interpalatine suture and the posterior part of the intermaxillary suture; only in one skull

Table 9 The distance between the greater palatine foramen and the midline maxillary suture according to sex and side

GPF-MMS	Sex				Total (N = 100) ($\bar{x}$ ± SD)	T	P
	Males (N = 64)		Females (N = 36)				
	Range	$\bar{x}$ ± SD	Range	$\bar{x}$ ± SD			
Right	11–16.3	14.87 ± 1.4	8.3–15.2	13.94 ± 2.1	14.25 ± 1.7	2.7	<0.05
Left	11.5–16.5	14.97 ± 1.2	8.3–15.5	13.96 ± 2.2	14.17 ± 1.6	2.6	<0.05
T	0.4		0.02		0.34		
P	>0.05		>0.05		>0.05		

GPF, greater palatine foramen; MMS, midline maxillary suture.

Table 10 The distance between the greater palatine foramen and the incisive foramen according to sex and side

GPF-IF (mm)	Sex				Total ($\bar{x}$ ± SD)	T	P
	Males		Females				
	Range	$\bar{x}$ ± SD	Range	$\bar{x}$ ± SD			
Right	30–41.5	37.09 ± 3.3	28.5–38	33.87 ± 2.89	35.93 ± 3.5	5.08	<0.001
Left	29.3–42.3	37.08 ± 3.7	29–40	34.19 ± 2.89	36.04 ± 3.7	2.89	<0.01
T	0.016		0.47		0.22		
P	>0.05		>0.05		>0.05		

GPF, greater palatine foramen; IF, incisive foramen.

Table 11 The distance between the greater palatine foramen and the posterior border of the hard palate according to sex and side

GPF-PBHP (mm)	Sex				Total ($\bar{x}$ ± SD)	T	P
	Males		Females				
	Range	$\bar{x}$ ± SD	Range	$\bar{x}$ ± SD			
Right	2.6–6.5	4.17 ± 0.94	2.7–5	3.39 ± 0.7	3.89 ± 0.9	4.71	<0.001
Left	2.6–6	4.2 ± 0.95	2.9–5.5	3.61 ± 0.7	3.99 ± 0.9	3.54	<0.01
T	0.18		1.33		0.79		
P	>0.0		>0.05		>0.05		

GPF, greater palatine foramen; PBHP, posterior border of the hard palate.

Figure 15

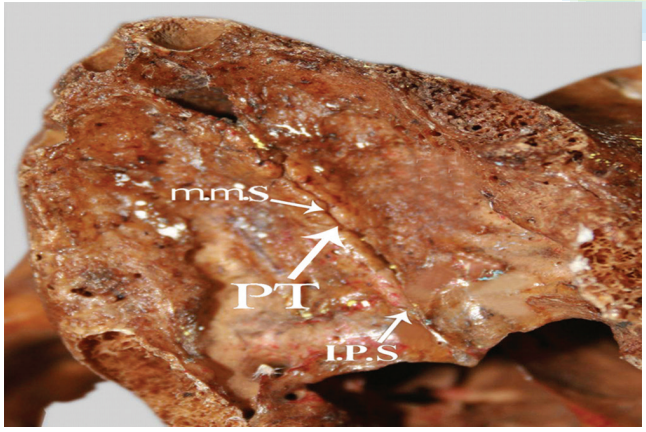

A photograph of an adult male skull. The hard palates have a palatine torus (PT) along the midline maxillary suture (MMS) and the anterior part of the interpalatine suture (IPS) in ridge form.

Figure 16

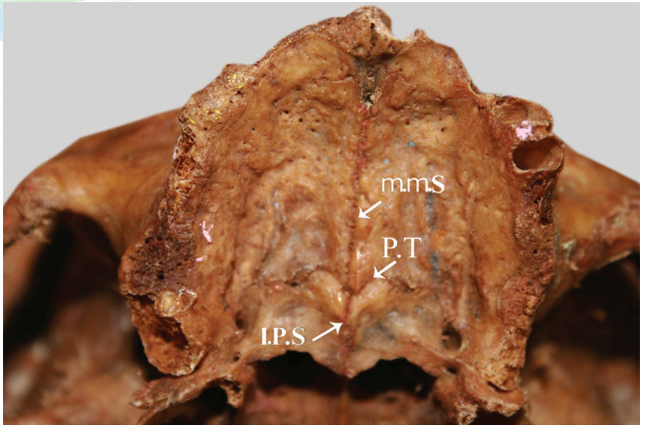

A photograph of an adult female skull. The hard palate has a palatine torus (PT) along the interpalatine suture (IPS) and the posterior part of the midline maxillary suture (MMS) in lump form.

did the palatine torus occupy the midpalatal suture and the anterior part of the interpalatine suture (Fig. 15).

The thickness of the palatal mucosa over the GPF in 20 cadaveric heads varied from 2 to 8.5 mm with a mean of 4.92 ± 1.93 mm (Fig. 17).

Discussions

In the present study, the mean palatal length was 52.77 ± 5.160 mm in male skulls and 49.66 ± 2.78 mm in female skulls, and the mean palatal breadth was 39.23 ± 3.02 and 37.7 ± 2.28 mm in male and female skulls, respectively. The average values of maximum palatal length and breadth in

Table 12 The distance between the greater palatine foramen and the hamular process of the pterygoid process according to both sides and sex

GPF-PtH (mm)	Sex				Total (N = 100) ($\bar{x}$ ± SD)	T	P
	Males (N = 64)		Females (N = 36)				
	Range	$\bar{x}$ ± SD	Range	$\bar{x}$ ± SD			
Right	6.5–16.8	12.29 ± 2.57	8–13.8	11.66 ± 1.57	12.06 ± 2.3	1.52	>0.05
Left	6.5–16.3	12.38 ± 2.45	7.5–13	11.51 ± 1.95	12.07 ± 2.2	1.9	>0.05
T	0.2		0.41		0.03		
P	>0.05		>0.05		>0.05		

GPF, greater palatine foramen; PtH, pterygoid process.

Table 13 The value of angle between the palatal midline and the line joining the greater palatine foramen and the incisive foramen (GIM) according to sex and side

GIM angle (deg.)	Sex				Total ($\bar{x}$ ± SD)	T	P
	Males		Females				
	Range	$\bar{x}$ ± SD	Range	$\bar{x}$ ± SD			
Right	16–34	23.3 ± 4.5	17–32	22.9 ± 4.4	22.9 ± 4.4	0.46	>0.05
Left	18–32	23.6 ± 3.9	17–32	23.1 ± 4.4	23.2 ± 4.1	0.59	>0.05
T	0.4		0.2		0.21		
P	>0.05		>0.05		>0.05		

Table 14 The value of the angle between the axis of the greater palatine canal and the hard palate (angle II) according to sex and side

Angle II (deg.)	Sex				Total ($\bar{x}$ ± SD)	T	P
	Males		Females				
	Range	$\bar{x}$ ± SD	Range	$\bar{x}$ ± SD			
R t	29–58	40.81 ± 9.1	22–56	39.89 ± 9.4	40.48 ± 9.1	0.48	>0.05
Left	28–60	40.69 ± 9.1	25–57	39.33 ± 9.4	40.2 ± 9.2	0.7	>0.05
T	0.075		0.25		0.22		
P	>0.05		>0.05		>0.05		

Table 15 Length of the greater palatine canal plus the length of the pterygopalatine fossa (greater palatine canal + pterygopalatine fossa) according to sex and side

GPF+PPF (mm)	Sex				Total ($\bar{x}$ ± SD)	T	P
	Males		Females				
	Range	$\bar{x}$ ± SD	Range	$\bar{x}$ ± SD			
Right	24.5–35.5	29.83 ± 3.2	22–32	28.61 ± 2.8	29.39 ± 3.1	1.99	<0.05
Left	24–35.5	29.99 ± 3.27	22–32.5	28.63 ± 29	29.5 ± 3.2	2.13	<0.05
T	0.28		0.3		0.25		
P	>0.05		>0.05		>0.05		

GPF, greater palatine foramen; PPF, pterygopalatine fossa

Table 16 The distance from the infraorbital foramen to the alveolar crest between the maxillary premolars (height of the maxilla) according to sex and bilaterally

Height of maxilla (mm)	Sex				Total ($\bar{x}$ ± SD)	T	P
	Males		Females				
	Range	$\bar{x}$ ± SD	Range	$\bar{x}$ ± SD			
Right	26–38	31.36 ± 3.37	24–34	28.82 ± 2.71	30.44 ± 3.4	4.11	<0.001
Left	26.5–37.5	31.63 ± 3.1	25–33	29.63 ± 2.5	30.91 ± 3.1	3.52	<0.01
T	0.47		1.32		1.02		
P	>0.05		>0.05		>0.05		

male skulls was significantly higher than those in female skulls (P < 0.001). Patel [9] found that the average maximum palatal length in male and female skulls was 50.28 ± 3.86 and 47.95 ± 3.68 mm, respectively, and the average maximum palatal breadth in male and female skulls was 37.17 ± 2.88 and 35.50 ± 3.07 mm in central India. The average maximum palatal length and breadth in male skulls in his study was significantly higher when compared with female skulls (P < 0.001).

Table 17 Variation in the diameters of the palatine torus in male and female skulls

Parameters	Length (mm)			Width (mm)			Height (mm)		
	Male	Female	Total	Male	Female	Total	Male	Female	Total
$\bar{x}$ ± SD	22.5 ± 10.5	18 ± 1.7	20.6 ± 7.8	9.9 ± 4.4	11.3 ± 5.5	10.5 ± 4.5	4.8 ± 1.3	3.3 ± 0.58	4.1 ± 1.2
Range	12–37	17–20	12–37	6.5–16	5–15	5–16	3–6	3–4	3–6
T	0.7			0.4			1.7		
P	>0.05			>0.05			>0.05		

Table 18 The percentage of form of the palatine torus in male and female skulls

Forms	Male [*N* (%)]	Female [*N* (%)]	Total [*N* (%)]
Ridge	2 (50)	1 (33.33)	3 (42.86)
Mound	2 (50)	1 (33.33)	3 (42.86)
Lump	0 (0.00)	1 (33.33)	1 (14.29)

Figure 17

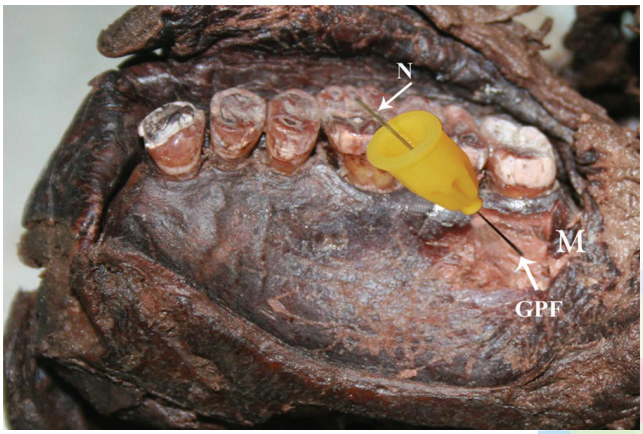

A photograph of a hard palate in a cadaver. The mucosa (M) over the greater palatine foramen (GPF) is reflected and a needle is inserted into the greater palatine canal through the GPF.

Gangrade *et al.* [10] found that the mean palatal length in male and female skulls was 54.59 and 52.44 mm, respectively. The palatal breadth in male and female skulls was38.49 and 35.89 mm, respectively; statistical analysis showed a significantly higher value of palatal length and breadth in male skulls compared with female skulls. The mean palatal length and breadth are sexually dimorphic. This finding is similar to that of Bigoni *et al.* [11] who noted significant sex differences in the region of the palate. Sumati *et al.* [12] also concluded that the size of the palate was the best sex determinant among five hard palate variables, and hard palate variables correctly classified sex in 70% of his sample from the North Indian population (Table 19).

This study found that 64% of Egyptian skulls had narrow palates (leptostaphyline), 12% had wide palates (brachystaphyline), and the remaining 24% had intermediate (mesostaphyline) palates, with no significant difference between the two sexes. In a study on Kenyan skulls by Hassanali and Mwaniki [7], 43% had narrow palates, 33% had wide palates, and 24% had intermediate palates. D'Souza *et al.* [13] found in South Indian skulls that 37.5% of the palates were narrow, 40% were wide, and 22.5% were intermediate. In this study, low palates were more in male skulls than in female skulls and the difference was significant. In the total sample, 56% had intermediate arched palates (orthostaphyline), 36% had low palates (chamestaphyline), and 8% had highly arched palates (hypsistaphyline).

When the results of this study were compared with the results of Saralaya and Nayak [14] on Indian skulls, it was found that the percentage of low palates was nearly similar in both studies, as it was 37.1% in Indian skulls. The percentage of highly arched palatal vaults was higher, at 16.7%. In Indian skulls, 46.2% showed an intermediate arched palate. D'Souza *et al.* [13] found that 87.5% of skulls had low palates and 12.5% had intermediate ones.

In the present study, the shape of the GPF was oval in 71 and 69% of skulls on the right and left sides, respectively. Cheung *et al.* [15] found an oval-shaped GPF in 82.4% of Chinese skulls. The average transverse diameter of the GPF was found to be 3.025 and 3.28 mm for right and left sides, respectively, in males and 2.6 and 2.4 mm for right and left sides, respectively, in females, with a highly significant difference between males and females. Compared with the results of Methathrathip *et al.* [4], the foramen diameter in this study was slightly longer.

The greater palatine neurovascular bundle gains an intraoral entry through the GPF, which thus merits caution during any palatal surgery. Excessive resistance while trying to negotiate the GPC could well be a consequence of the inability of the clinician to accurately locate the GPF. In contrast, a common error observed while attempting the GPC approach to the maxillary nerve is the needle stepping off the posterior aspect of the hard palate, in which cases the anesthetic would be deposited in the nasopharynx [16]. Clinicians should suspect the latter if there is a complete lack of resistance to the advancing needle. It is thus imperative that the position of the foramen be defined relative

to intraoral reference points, which are readily identified in a living patient.

The majority of the studies conducted to observe the location of the GPF (Table 2) found it to be opposite the third molar tooth in 70–80% of the samples. Sujatha *et al.* [17] observed this location in 85.95% of Indian skulls, whereas Wang *et al.* [20] reported the same location in only 33.5% of Chinese skulls.

The present study found the GPF to be opposite the upper maxillary third molar tooth in the majority of skulls (84%). It also showed that the location of GPF was intermediate between the second and the third molars in 9% of the sample, distal to the maxillary third molar in 6%, and opposite the upper second molar tooth in 1% (Table 20).

In the present study, the mean distance of the GPF from the MMS was 14.25 mm on the right side and 14.17 mm on the left side, which fell slightly below previous established averages (Table 21). The highest average was in Thai skulls, which was 16.20 mm. As far as the symmetry of position of the GPF from the MMS on both sides is concerned, the results of this study were similar to those of Chrcanovic and Custódio [2] and Sharma and Garud [19] in that the position was almost the same on both sides. Teixeira [21] demonstrated a significant difference between the two sides in Brazilian skulls. Methathrathip *et al.* [4] and Teixeira [21] found a statistically significant intersex difference in the distance between the GPF and MMS, which was in agreement with the results of this study.

Table 19 Comparison of data from the literature on the mean distance of palatal length and breadth in mm

References	Race	Length in males	Length in females	Breadth in males	Breadth in females
Gangrade *et al.* [10]	–	54.59	52.44	38.49	35.89
Patel [9]	Central Indian	50.28	47.95	37.17	35.50
This study	Egyptian	52.77	49.66	39.23	37.71

The mean distance of the GPF from the posterior palatal border was highly variable in previous studies (Table 21).

Westmoreland and Blanton [22] documented an average distance of 1.9 mm. Malamed and Treiger [16] found the mean value to be 6.97 mm. The corresponding mean value in the present study was 3.89 mm on both sides. Given the disparity in the reported values of this parameter among various studies (Table 21), the authors inferred that no conclusive figure could be advocated for this distance.

In the present study, the distance from the tip of the hamular process to the GPF was 12.06 mm in comparison with the findings of Malamed and Trieger [16] (12 mm) and Sharma and Garud [19] (11.78 mm). The pterygoid hamulus bears a consistent relationship to the GPF in the sagittal plane. Therefore, the authors maintain the possibility of using the palpable hamulus for accurate location of the GPF.

The distance between the GPF and the incisive fossa was 35.93 mm on the right side and 36.04 mm on the left side, which is close to the previous results of Shama and Garud [19] (35.42 mm), Chrcanovic and Custódio [2] (right side 36.2 mm, left side 36.5 mm), and Saralaya and Nayak [14] (right side 37.2 mm, left side 37.2 mm).

This distance showed a significant difference between the two sexes, which was in agreement with the results of Nascimento Correia Lima *et al.* [24] (Table 22).

In the present study, the mean angle between the MMS and the line from the IF and the GPF was almost equal on both sides (22.9° on the right side and 23.2° on the left side). Saralaya and Nayak [14] found this angle to be 21.1° on the right side and 21.2° on the left side. In the study by Chrcanovic and Custódio [2] the angle was 22.7° in Brazilian skulls. Knowledge of the mean value of this angle would help professionals to determine the angle to be made

Table 20 Comparison of data on the positional variance of the greater palatine foramen with respect to the maxillary molar

References	Race	Opposite third molar (%)	Between second and third molar (%)	Opposite second molar (%)	Distal to third molar (%)
Methathrathip *et al.* [4]	Thais	64.40	23.10	5.60	6.90
Chrcanovic and Custódio [2]	Brazilian	54.80	6.91	0	38.94
Hassanali and Mwaniki [7]	Kenyan	76	13.60	10.40	0
D'Souza *et al.* [13]	South Indian	73.75	23.75	2.5	0
Saralaya and Nayak [14]	Indian	74.60	24.20	0.40	0.80
Sujatha *et al.* [17]	Indian	85.95	–	–	–
Piagkou *et al.* [18]	Greek	76.2	–	–	–
Sharma and Garud [19]	Western India	73.38	0	8.63	17.99
Wang *et al.* [20]	Chinese	33.5	–	17	–
This study	Egyptian	84	9	2	6

Table 21 Comparison of data from the literature on the mean distance from greater palatine foramen to midline maxillary suture and posterior palatine border in mm

References	Race	GPF-MMS	GPF-PPB
Jaffar and Hamadah [23]	Caucasoid	15.71	4.86
Methathrathip *et al.* [4]	Thias	16.20	5.10
Saralaya and Nayak [14]	Indian	14.70	4.20
Chrcanovic and Custódio [2]	Brazilian	14.68 (R), 14.44 (L)	3.39
Piagkou *et al.* [18]	Greek	15.3	4.6 (R), 4.7 (L)
Sharma and Garud [19]	Western India	14.71 (R), 14.41 (L)	3.42 (R), 3.38 (L)
Westmorel and and Blanton [22]	–	14.8 (R), 15 (L)	1.90
Malamed and Trieger [16]	–	–	6.97
This study	Egyptian	14.25 (R), 14.17 (L)	3.89 (R), 3.99 (L)

GPF, greater palatine foramen; L, left; MMS, midline maxillary suture; R, right.

Table 22 Comparison of data from the literature on the mean distance from the greater palatine foramen to the incisive fossa and from the greater palatine foramen to the pterygoid hamular processes (mm)

References	Race	GPF-IF	GP-PH
Saralaya and Nayak [14]	Indian	37.2 (R), 37.2 (L)	–
Chrcanovic and Custódio [2]	Brazilian	36.21 (R), 36.52 (L)	–
Sharma and Garud [19]	Western India	35.42 (R), 35.66 (L)	11.78
Malamed and Trieger [16]	–	–	12
Nascimento Correia Lima *et al.* [24]	Brazilian	41.00	–
This study	Egyptian	35.93 (R), 36.04 (L)	12.06 (R), 12.07 (L)

GPF, greater palatine foramen; L, left; IF, incisive foramen; R, right.

by the needle for anesthetic infiltration into the GPF. When using the GPC approach for maxillary nerve block, it is important to have knowledge of the length of the GPC+PPF. Although unusually long canals could lead to a lack of anesthesia, short canals could be hazardous because of overpenetration, which might result in an intraorbital or intracranial injection. The distance from the IOF to the alveolar crest between the maxillary bicuspids corresponds well to the length of the GPC+PPF [25]. The mean value of this measurement was 29.39 and 29.83 mm on the right and left sides, respectively, similar to the results of Sharma and Garud [19], who found it to be equal to 29.22 mm, which was considerably lower than that noted by Malamed and Trieger [16] (mean 32.15 mm). Bharadwaj and Novotny [26] have advocated the safe extent of penetration to be in the range of 22.25 mm, taking into account the inconsistency in values noted by various authors, which could possibly be due to the multiethnic origin of the various skull samples studied. In the present study, the mean thickness of the palatal mucosa over the GPF was 5.92 mm. This is nearly similar to the results of Methathrathip *et al.* [4], who found the thickness of the mucosa over the GPF in Thai cadavers to be 6.7 mm. Therefore, the estimated length of needle to be inserted through the GPF toward the foramen rotundum should be the length of GPC and PPF combined with the thickness of the palatal mucosa over the GPF.

Palatal tori are usually a clinical finding with no treatment necessary. It is possible for ulcers to form on the area of the tori because of repeated trauma. Also, the tori may complicate the fabrication of dentures [8].

In the present study, the percentage of palatine tori was 7% overall. Hassanali and Mwaniki [7] found palatine torus in 4.8% of Kenyan skulls. Zivanovic [27] found the torus to be present in 33.5% of males and 49.06% of females in the Galloway collection. Kellock and Parsons [28] found the incidence of the palatine torus to be 4.5% in Australian aborigines, 5.1% in Polynesians, and absent in the Melanesian cranial sample.

Sapp *et al.* [29] found the torus in at least 3% of adults and it was more common in females than in males in their study.

In the present study, the position of the torus was along the median palatine suture and was of medium size. These results are similar to the results of Skrzat *et al.* [30].

Acknowledgements
Nil.

Financial support and sponsorship
Nil.

Conflicts of interest
There are no conflicts of interest.

References

1 Burris BG, Harris EF. Identification of race and sex from palate dimensions. J Forensic Sci 1998; **43**:959 –963.

2 Chrcanovic BR, Custódio AL. Anatomical variation in the position of the greater palatine foramen. J Oral Sci 2010; **52**:109–113.

3 Malamed SF. *Handbook of local anesthesia*. 5th ed. St. Louis: Elsevier Mosby; 2004.

4 Methathrathip D, Apinhasmit W, Chompoopong S, Lertsirithong A, Ariyawatkul T, Sangvichien S. Anatomy of greater palatine foramen and canal and pterygopalatine fossa in Thais: considerations for maxillary nerve block. Surg Radiol Anat 2005; **27**:511–516.

5 Howard-Swirzinski K, Edwards PC, Saini TS, Norton NS. Length and geometric patterns of the greater palatine canal observed in cone beam computed tomography. Int J Dent 2010; **2010**:143–149.

6 Standring S, Ellis H, Healy JC, Johnson D, Williams A, Collins P, Wigley C. *Gray's anatomy*. 40th ed. Edinburgh: Elsevier Churchill Livingstone; 2008. **4**:502–503.

7 Hassanali J, Mwaniki D. Palatal analysis and osteology of the hard palate of the Kenyan African skulls. Anat Rec 1984; **209**:273–280.

8 Chochayeb AA, Volpe AR. Occurrence of torus palatines and mandibularis among women of different ethnic group. Am J Dent 2001; **14**:278–280.

9 Patel M. A study of the hard palate in the skull of central Indian population. Int J Pharm Biosci 2012; **3**:572.

10 Gangrade P, Babel H, Saini R, Vyas A. Sexing of skull through the morphometric of hard palate. Int J Curr Res Rev 2012; **4**:168.

11 Bigoni L, Veleminska J, Bruzek J. Three dimensional geometric morphometric analysis of cranio-facial sexual dimorphism in a central European sample of known sex. Homo 2010; **61**:16–32.

12 Sumati, Patnaik VVG, Phatak A. 2012): Determination of sex from hard palate by discriminant function analysis. Int J Basic Appl Med Sci **2**:243–251.

13 D'Souza AS, Mamatha H, Nayak J. Morphometric analysis of hard palate in south Indian skulls. Biomed Res 2012; **23**:173–175.

14 Saralaya V, Nayak SR. The relative position of the greater palatine foramen in dry Indian skulls. Singapore Med J 2007; **48**:1143–1146.

15 Cheung LK, Fung SC, Li T, Samman N. Posterior maxillary anatomy: implications for Le Fort I osteotomy. Int J Oral Maxillofac Surg 1998; **27**:346–351.

16 Malamed SF, Trieger N. Intraoral maxillary nerve block: an anatomical and clinical study. Anesth Prog 1983; **30**:44–48.

17 Sujatha N, Manjunath KY, Balasubramanyam V. Variations of the location of the greater palatine foramina in dry human skulls. Indian J Dent Res 2005; **16**:99 –102.

18 Piagkou M, Xanthos T, Anagnostopoulou S, Demesticha T, Kotsiomitis E, Piagkos G, et al.. Anatomical variation and morphology in the position of the palatine foramina in adult human skulls from Greece. J Craniomaxillofac Surg 2012; **40**:206–210.

19 Sharma NA, Garud RS. Greater palatine foramen-key to successful hemimaxillary anesthesia: a morphometric study and report of a rare aberration. Singapore Med J 2013; **54**:152–159.

20 Wang TM, Kuo KJ, Shih C, Ho LL, Liu JC. Assessment of the relative locations of the greater palatine foramen in adult Chinese skulls. Acta Anat (Basel) 1988; **132**:182–186.

21 Teixeira CS. Topography of the greater palatine foramen in macerated skull. University of Brasilia:Brasilia:Health Science 2007.58. [Master's thesis in health science].

22 Westmoreland EE, Blanton PL. An analysis of the variations in position of the greater palatine foramen in the adult human skull. Anat Rec 1982; **204**:383–388.

23 Jaffar AA, Hamadah HJ. An analysis of the position of the greater palatine foramen. J Basic Med Sci 2003; **3**:24–32.

24 Nascimento Correia Lima N, Fortes de Oliveira O, Sassi C, Picapedra A, Francesquini L Jr, Daruge E Jr. Sex determination by linear measurements of palatal bones and skull base. J Forensic Odontostomatol 2012; **30**:38–44.

25 Hawkins JM, Isen D. Maxillary nerve block: the pterygopalitine canal approach. J Calif Dent Assoc 1998; **26**:658–664.

26 Bharadwaj VK, Novotny GM. Greater palatine canal injection: an alternative to the posterior nasal packing and arterial ligation in epistaxis. J Otolaryngol 1986; **15**:94–100.

27 Zivanovic S. Longitudinal grooves and canals of the human hard palate. Anat Anz 1980; **147**:161–167.

28 Kellock WL, Parsons PA. A comparison of the incidence of minor nonmetrical cranial variants in Australian aborigines with those of Melanesia and Polynesia. Am J Phys Anthropol 1970; **33**:235–240.

29 Sapp JP, Eversole LR, Wysocki GP. *Contemporary oral and maxillofacial pathology*. St. Louis: Mosby; 1997. 433.

30 Skrzat J, Holiat D, Walocha J. Themorpholodical appearance of the palatine tours in the cracovian skulls (XV–XVIII century). Folia Morphol 2003; **62**:183–186.